NASA TECHNICAL NOTE

NASA TN D-3752

NASA TN D-3752

c. 1

INTERACTION EFFECTS OF A CONTROL JET EXHAUSTING RADIALLY FROM THE NOSE OF AN OGIVE-CYLINDER BODY AT TRANSONIC SPEEDS

by Edwin E. Lee, Jr., and Conrad M. Willis

Langley Research Center
Langley Station, Hampton, Va.

NATIONAL AERONAUTICS AND SPACE ADMINISTRATION • WASHINGTON, D. C. • JANUARY 1967

NASA TN D-3752

INTERACTION EFFECTS OF A CONTROL JET EXHAUSTING RADIALLY FROM THE NOSE OF AN OGIVE-CYLINDER BODY AT TRANSONIC SPEEDS

By Edwin E. Lee, Jr., and Conrad M. Willis

Langley Research Center
Langley Station, Hampton, Va.

NATIONAL AERONAUTICS AND SPACE ADMINISTRATION

For sale by the Clearinghouse for Federal Scientific and Technical Information
Springfield, Virginia 22151 – Price $2.00

INTERACTION EFFECTS OF A CONTROL JET EXHAUSTING RADIALLY FROM THE NOSE OF AN OGIVE-CYLINDER BODY AT TRANSONIC SPEEDS

By Edwin E. Lee, Jr., and Conrad M. Willis
Langley Research Center

SUMMARY

An investigation has been conducted to determine the influence of the main airstream upon the control effectiveness of a nose-mounted control jet exhausting radially from an ogive-cylinder body. The control jet was operated at jet total pressures of up to 560 psia $(3861 \times 10^3$ newtons/meter$^2)$. Tunnel Mach number ranged from 0.60 to 1.05 with angles of attack ranging from -4° to 8°. Average Reynolds number was 3.8×10^6 per foot $(12.5 \times 10^6$ per meter$)$.

The pitching moments produced by the control jet were reduced by interactions with the main airstream at all test conditions. The amount of control-moment reduction varied from about 30 to 55 percent of the moment produced by the jet exhausting into quiescent air.

INTRODUCTION

Reaction controls provide a simple and convenient means of maintaining a desired attitude and flight path for high-speed vehicles. When control jets are operated within the atmosphere the net force applied to the vehicle may be influenced by interactions between the jet, the external stream, and the vehicle surfaces. A considerable amount of research, both analytical and experimental, has been done on the interaction between the free stream and a jet directed at right angles to it (refs. 1 to 7). However, most of the research has been for the case in which the control jets were located in the rearward half of the body (Scout vehicle, for example).

In some cases design problems arise that would be alleviated if the control jets could be moved to a more forward location. Some of these problems are base recirculation, length of moment arm for the applied control thrust, interference with the reception and transmission of data, and space considerations. Also, with nose-located control jets, the jet reaction force that accompanies pitch and yaw control moments reinforces changes in aerodynamic forces generated by changes in angle of attack, while jets aft of the vehicle center of gravity result in the opposite effect, or opposing forces.

This paper presents results of tests to determine interaction effects of the main airstream with a radially exhausting control jet mounted in the nose of a missile. The model for this investigation was an ogive-cylinder 39.12 inches (99.36 cm) long with a pitch control jet at model station 4.75 (12.07 cm). A hot jet exhaust, produced by decomposing concentrated hydrogen peroxide (90 percent), was operated at ratios of jet total pressure to free-stream static pressure up to 65. The free-stream Mach number was varied from 0.60 to 1.05.

SYMBOLS

The physical quantities used in this report are given in U.S. Customary Units and in the International System of Units. Definitions of the latter, as well as factors relating the two systems of units, are given in reference 8.

A maximum cross-sectional area of model, in^2 (m^2)

C_F control-jet thrust coefficient, F/qA

C_m pitching-moment coefficient about model station 21.0 (53.34 cm), $\frac{\text{Pitching moment}}{qAd}$

ΔC_m change in pitching-moment coefficient due to jet operation, $(C_m)_{jet\text{-}on} - (C_m)_{jet\text{-}off}$

C_{m_α} slope of pitching-moment curve at zero angle of attack, $\frac{\partial C_m}{\partial \alpha}$ per deg

C_N normal-force coefficient, $\frac{\text{Normal force}}{qA}$

ΔC_N change in normal-force coefficient due to jet operation, $(C_N)_{jet\text{-}on} - (C_N)_{jet\text{-}off}$

C_{N_α} slope of normal-force curve at zero angle of attack, $\frac{\partial C_N}{\partial \alpha}$ per deg

C_p pressure coefficient, $\frac{p_l - p_\infty}{q}$

d	diameter of model, in. (cm)
F	control-jet thrust, lb (N)
M	free-stream Mach number
p	pressure, psia (N/m^2)
q	free-stream dynamic pressure, psia (N/m^2)
x	model station, measured positive rearward from nose of model, in. (cm)
$\bar{x}$	longitudinal distance from moment center to jet-nozzle center line, in. (cm)
α	model angle of attack, deg
K_m	control-jet pitching-moment effectiveness, $\dfrac{\Delta C_m}{C_F \frac{\bar{x}}{d}}$
K_N	control-jet normal-force effectiveness, $\dfrac{\Delta C_N}{C_F}$
θ	meridian angle, positive clockwise from top when looking upstream, deg

Subscripts:

b	base of model
c	control-motor chamber
l	local
∞	free stream

Conversion factors for the specific quantities used in this paper are given in the following table:

$$1 \text{ psi} = 6.8947572 \times 10^3 \text{ newtons/meter}^2$$
$$1 \text{ inch} = 2.54 \text{ centimeters}$$
$$1 \text{ inch}^2 = 6.4516 \times 10^{-4} \text{ meters}^2$$

1 pound force = 4.448221615 newtons

1 in-lbf = 0.112984829 meter-newtons

^{o}K = $(5/9)(^{o}F + 459.67)$

APPARATUS AND MODEL

The investigation was conducted in the Langley 16-foot transonic tunnel, an octagonal, slotted-throat, single-return, wind tunnel operated at atmospheric stagnation pressures. A sketch and a photograph of the model are presented in figures 1 and 2. The sting-mounted model was 39.12 inches (99.36 cm) long and 6.00 inches (15.24 cm) in diameter. An ogive nose with a hemispherical tip was faired into a cylindrical section at model station 9.70 (24.64 cm). A pitch control jet was mounted in the ogive nose section at model station 4.75 (12.07 cm). The jet nozzle had a throat diameter of 0.271 inch (0.688 cm) and an area ratio of 3.25. An activated silver-screen catalyst pack in the motor decomposed hydrogen peroxide (90 percent concentration) to provide the hot jet exhaust. The nozzle center line was at right angles to the model center line with the nozzle exit plane slightly inside the body contour. A second nozzle, fed by a separate motor, was located 1/2 inch (1.77 cm) behind the pitch nozzle and rotated 90^{o} for yaw control. After preliminary tests to determine interference effects between the two jets, the yaw-motor propellant line was removed and the nozzle plugged.

A six-component strain-gage balance mounted inside the model measured forces and moments about the model moment center at station 21.00 (53.34 cm). Pressure distributions over the model were sensed by a single transducer connected to a pressure-sampling valve that stepped from one orifice to the next at a rate of eight pressure measurements per second. Model angle of attack was measured by a strain-gage inclinometer mounted in the nose.

TESTS

The tests were conducted in the Langley 16-foot transonic tunnel. Mach numbers ranged from 0.60 to 1.05. Data were obtained at eight angles of attack ranging from -4^{o} to 8^{o} for each of the five test Mach numbers. A jet-off data point was taken immediately before and after each jet-on data point. The jet was operated at thrust levels of 20 and 40 pounds (89 and 178 newtons) over the complete test range, and at several additional intermediate thrust levels at a Mach number of 0.90 only. Pressure data and force data to show the interaction between two jets were obtained at the beginning of the test; then the pressure tubing and the second motor were removed to reduce force-balance restraint before the single-jet data were obtained. Jet total pressure ranged from 250 to 560 psia

(1724×10^3 to 3861×10^3 newtons/meter^2) and total temperature of the exhaust was about 1365° F (1019° K). The tunnel Reynolds number was about 3.8×10^6 per foot (12.5×10^6 per meter). There was no fixed transition.

A static calibration of the jet motor was obtained before testing in the presence of an external stream. Comparison of force data from motor-alone and complete-model tests (fig. 3) shows no interaction effects between model and jet at zero Mach number, and this finding was confirmed by body pressure distributions (not shown). Jet thrust for the test points with the tunnel operating was calculated by using the measured chamber pressure and static calibration data and correcting for the ambient pressure of the wind-tunnel airstream. Figure 4(a) shows the variation of jet total-pressure ratio with Mach number for constant values of jet thrust of 20 and 40 pounds (88.96 and 177.93 newtons), and figure 4(b) shows the variation of jet total-pressure ratio with thrust coefficient at $M = 0.9$.

ACCURACY

The accuracy of these data is estimated to be as follows:

C_F	±0.005
C_m	±0.013
C_N	±0.014
C_p	±0.02
M	±0.008
α, deg	±0.1

RESULTS AND DISCUSSION

The influence of control-jet operation on model surface pressures is indicated in figure 5. Pressure coefficients along the top and bottom of the model at a Mach number of 0.90 and angle of attack of 0° are shown with the jets off, and with the pitch jet operating singly and in combination with a yaw jet, at the 40-pound (178-newton) thrust level.

When the pitch jet was turned on, a relatively small stagnation region formed ahead of the nozzle, and local pressures increased above jet-off values. To the sides and rear of the nozzle opening, pressures were considerably lower than with the jet off, particularly in the dead wake region just behind the jet plume. Qualitatively, the jet obstructs and diverts the flow near the model surface somewhat like a rigid cylinder. From a quantitative standpoint, however, the gas jet causes a more extensive disturbance and lower pressures downstream than if it were a rigid cylinder. (See ref. 6.) The jet spreads, obstructing the flow more after leaving the nozzle, and entrains low-energy air from the adjacent surface as it penetrates the main flow and turns downstream. (See ref. 7.) Within 2 inches (5.08 cm) behind the control-jet exit low pressures extended laterally over most of the planform diameter of the nose (fig. 5(b), model station 6.6 (16.76 cm)). Farther downstream, noticeable pressure reductions also occurred along the bottom surface. Thus, the jet interference field was swept back and down around the sides of the model and was strong enough to disturb the flow over the entire circumference of the forebody. Flow over the rear two-thirds of the model was relatively unaffected by the jet, as shown by the body and base pressures in figures 5(a) and 6, respectively. The force data, discussed subsequently, show that the suction region induced on top of the nose was the predominant source of interference. It produced forces in opposition to the momentum thrust of the jet and reduced the effectiveness of the pitch-control motor appreciably.

Pitch and yaw jets were operated simultaneously to determine any "carryover" interference from the yaw control on forces in the pitch plane. The circumferential pressure distributions at stations just ahead of and behind the nozzle exits show no appreciable asymmetry or variation in level between single- and dual-control operation. This was true for at least 30° displacement from the pitch plane in the direction of the yaw jet (fig. 5(b)). Some further reduction in pressure did occur along the bottom of the model (fig. 5(a)); however, the corresponding force data, presented in figure 7, show that the net carryover effect was very small. Therefore it was concluded that pitching or yawing interference could be adequately determined by operating only one motor and varying the model attitude in the same plane. Consequently, the yaw motor, propellant line, and the pressure instrumentation as well, were removed to simplify the model installation, and the aerodynamic interference from the pitch jet alone was investigated more extensively.

Normal-force and pitching-moment coefficients are plotted against angle of attack in figure 8 for each test Mach number with the pitch jet off and with it operating at thrust levels of 20 and 40 pounds (89 and 178 newtons). The dashed curve indicates the force when the full 40-pound (178-newton) thrust and corresponding moment are added to the jet-off values without interference. A similar curve for the 20-pound (89-newton) thrust level was omitted for clarity, but may be readily visualized. By comparing the actual and interference-free data it is evident that large unfavorable jet-interference effects occurred at all test conditions. Adverse interference, in this case, is synonymous with induced force and moment increments in the positive direction, which in view of the pressure changes discussed previously can only be attributed to the suction induced on the top of the forebody behind the jet. At a Mach number of 0.90 only, longitudinal aerodynamic characteristics were also obtained for other thrust values generally intermediate to the 20- and 40-pound (89- and 178-newton) levels, and the results are plotted in figure 9 against thrust coefficient based on maximum body cross-sectional area. Figures 8 and 9 both indicate that jet interference, though definitely unfavorable, did not cause any erratic variations or large nonlinearities in the aerodynamic characteristics of the model over the range of conditions investigated.

Figure 10 summarizes the jet effects on the normal-force and pitching-moment derivatives with respect to angle of attack. These derivatives were evaluated at 0° angle of attack from the data in figure 8. Increasing the jet thrust generally increased C_{N_α}, and the difference between jet-off conditions and the 40-pound (178-newton) thrust level varied from 5 percent at low subsonic speeds to a maximum of 16 percent at a Mach number of 1.00. Jet operation reduced C_{m_α} approximately 5 percent at low subsonic speeds, but there was only a small effect of jet operation at Mach numbers greater than 0.90.

The effect of jet operation at a thrust of 40 pounds (178 newtons) on the model center-of-pressure location is shown in figure 11 for Mach numbers of 0.60 and 1.05. No momentum thrust or moment effects are included in these results, only jet-off aerodynamic forces plus jet interferences. The jet-off center-of-pressure location was practically independent of angle of attack and Mach number, but with the jet operating, the position shifted rearward as the angle of attack increased. The maximum travel was approximately 1.5 body diameters and occurred at a Mach number of 1.05.

The variations with angle of attack of jet normal-force and pitching-moment control effectiveness are presented in figures 12 and 13, respectively, for the 20- and 40-pound (89- and 178-newton) thrust levels. The values of K represent the fraction of motor reaction force or moment available for control. These values were computed by dividing the actual difference between the jet-on and jet-off data of figure 8 by the momentum thrust of the jet, or by the corresponding moment about the reference center of gravity.

The results show that jet effectiveness generally diminished with increasing Mach number. At 0° angle of attack, only about 45 to 70 percent of the reaction force and moment were available for control purposes throughout the Mach number range, regardless of thrust level. Increasing the angle of attack caused further reductions in K_N, particularly at transonic speeds, where values were as low as 0.20 (see fig. 12(a), $M = 1.05$). This trend may have been partly related to the body wake forming with increasing cross flow ($M \sin \alpha$). The corresponding reduction in flow energy behind the jet would tend to make the exhaust aspirate more extensively. Variations in the center-of-pressure location and the normal interference force were largely compensating, so that the moment effectiveness was not influenced significantly by attitude changes.

Values of K_N and K_m for the variable-thrust runs at a Mach number of 0.90 are plotted against thrust coefficient in figure 14. The jet effectiveness parameters increased with increasing thrust coefficient, but were quite low even at the highest thrust (pressure ratio) levels of this investigation. (Also compare figs. 12 and 13.)

SUMMARY OF RESULTS

An investigation of interaction effects on the control effectiveness of a jet exhausting perpendicular to the main airstream has been conducted in the Langley 16-foot transonic tunnel. The results can be summarized as follows:

1. The interaction between the nose-mounted jet and the free stream produced sizable pressure reductions on the body behind the nozzle. This effect generated forces opposite to the reaction thrust and reduced the jet control effectiveness appreciably.

2. Increasing either the free-stream Mach number or the angle of attack (jet exhausting upward) generally increased the jet interference.

3. The jet effectiveness parameters increased with increasing thrust coefficient, but were quite low even at the highest thrust (pressure ratio) levels of this investigation.

Langley Research Center,
National Aeronautics and Space Administration,
Langley Station, Hampton, Va., August 3, 1966,
126-13-01-04-23.

REFERENCES

1. Ferrari, Carlo: Interference Between a Jet Issuing Laterally From a Body and the Enveloping Supersonic Stream. Bumblebee Rept. No. 286 (Contract NOrd 7386), Appl. Phys. Lab., Johns Hopkins Univ., Apr. 1959.
2. Kaufman, Louis G., II.: Classification of Interactions Due to High-Speed Flows Past Transverse Jets. Res. Rept. RE-154, Grumman Aircraft Eng. Corp., Feb. 1962.
3. Morkovin, M. V.; Pierce, C. A., Jr.; and Cravan, C. E.: Interaction of a Side Jet With a Supersonic Main Stream. Bull. No. 35, Eng. Res. Inst., Univ. of Michigan, Sept. 1952.
4. Vinson, P. W.; Amick, J. L.; and Liepman, H. P.: Interaction Effects Produced by Jet Exhausting Laterally Near Base of Ogive-Cylinder Model in Supersonic Main Stream. NASA MEMO 12-5-58W, 1959.
5. Amick, James L.; and Hays, Paul B.: Interaction Effects of Side Jets Issuing From Flat Plates and Cylinders Alined With a Supersonic Stream. WADD Tech. Rept. 60-329, U.S. Air Force, June 1960.
6. Vogler, Raymond D.: Surface Pressure Distributions Induced on a Flat Plate by a Cold Air Jet Issuing Perpendicularly From the Plate and Normal to a Low-Speed Free-Stream Flow. NASA TN D-1629, 1963.
7. Jordinson, R.: Flow in a Jet Directed Normal to the Wind. R. & M. No. 3074, British A.R.C., 1958.
8. Mechtly, E. A.: The International System of Units – Physical Constants and Conversion Factors. NASA SP-7012, 1964.

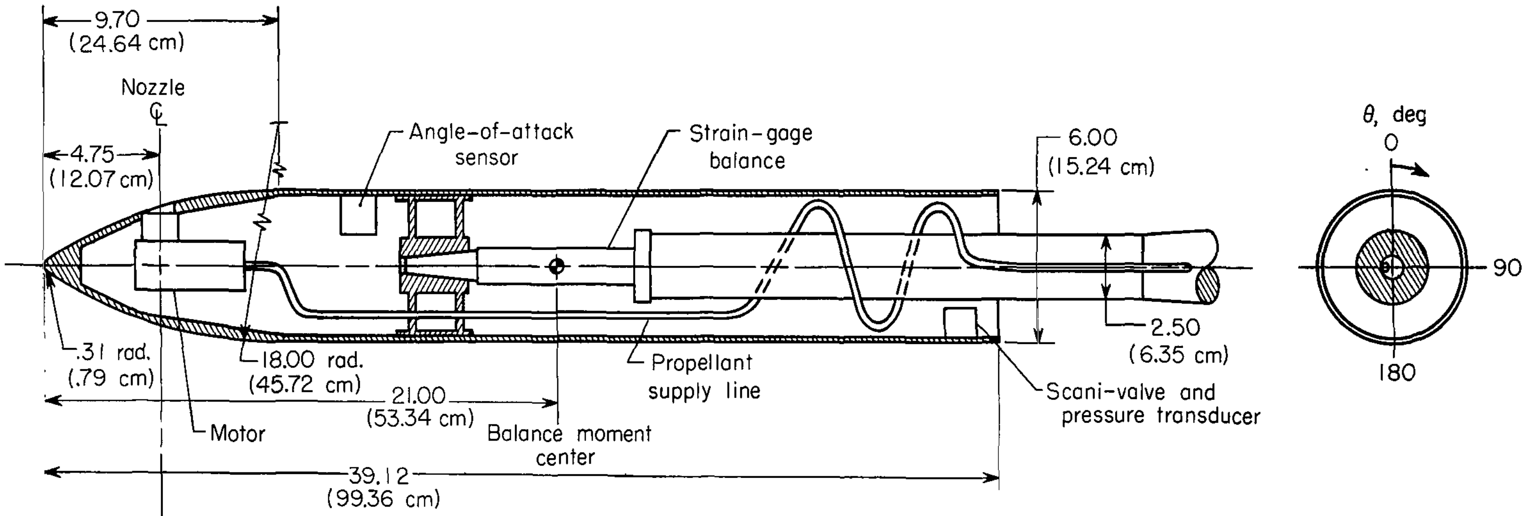

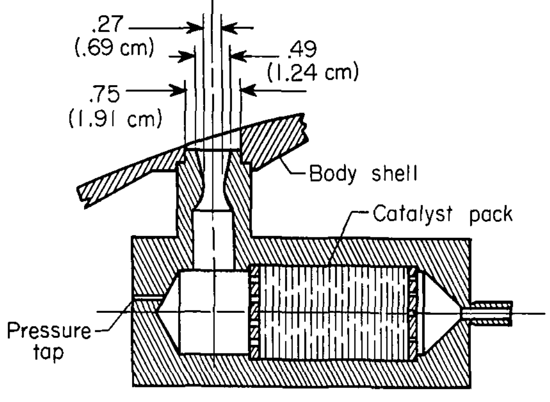

Motor and nozzle details

Orifice locations		
Model station		θ, deg
cm	in.	
9.14	3.60	0, 180
10.16	4.00	-26, -12, 0, 12, 26
10.16	4.00	154, 168, 180, 192, 206
13.72	5.40	0
14.99	5.90	0, 180
16.76	6.60	-45, -26, -12, 0, 26
16.76	6.60	154, 168, 180, 192, 206, 225
19.56	7.70	0, 180
23.11	9.10	0, 180
27.69	10.90	0, 180
38.61	15.20	0, 180
55.88	22.00	0, 180
85.60	33.70	0, 180

Figure 1.- Sketch of the model and control rocket. All dimensions are in inches unless otherwise noted.

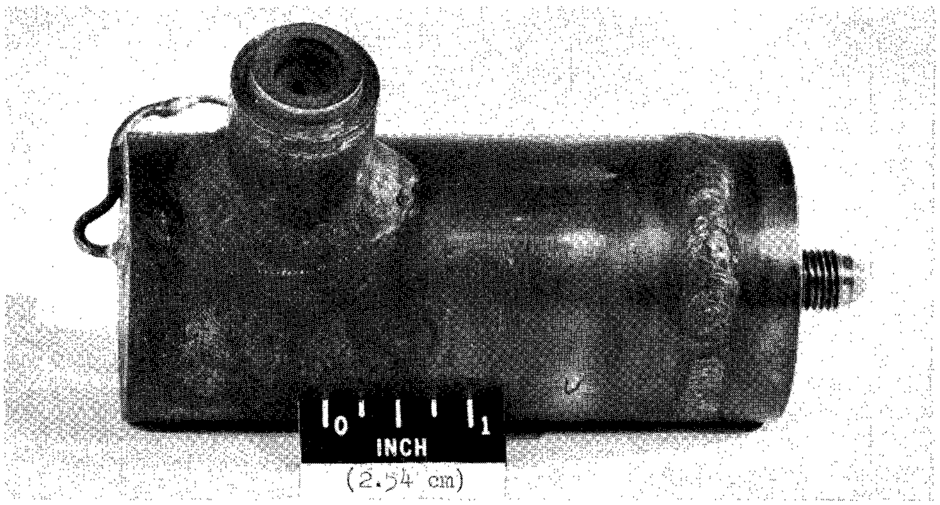

(a) Pitch or yaw control rocket. L-62-6065

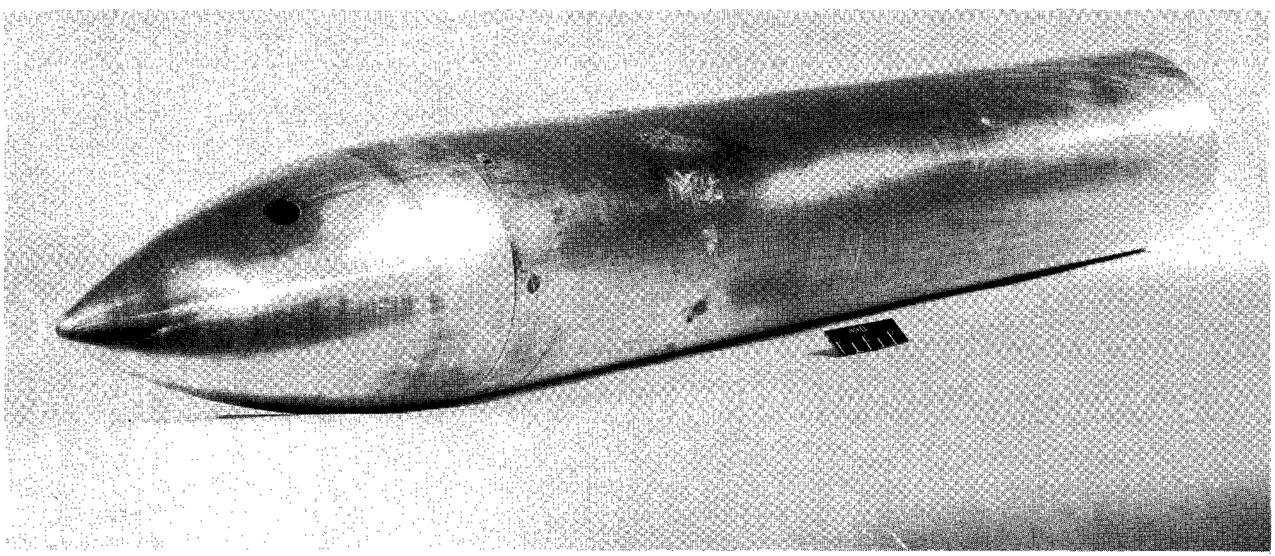

(b) Ogive-cylinder model. L-62-6067

Figure 2.- Model and hydrogen-peroxide-fueled control rockets.

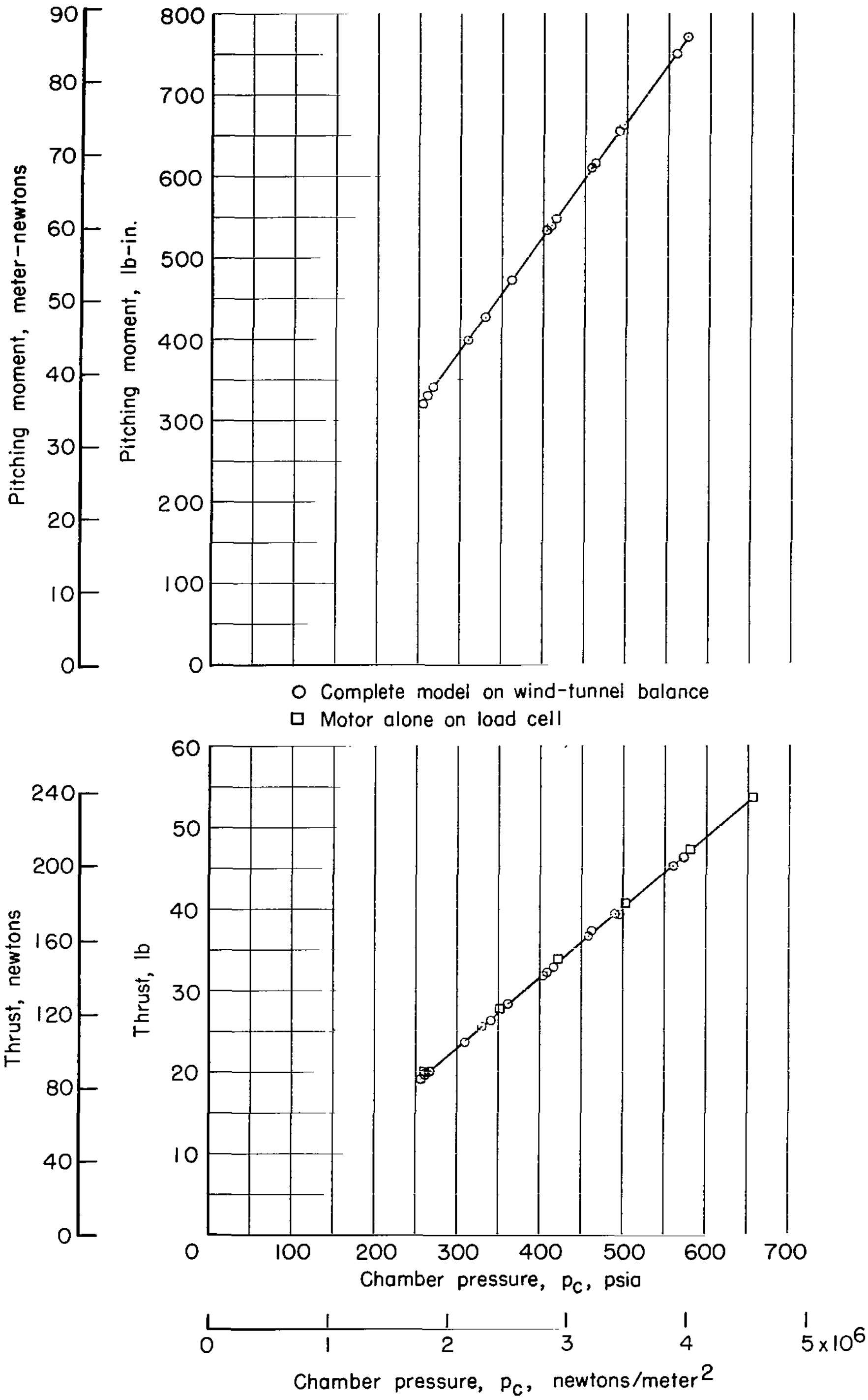

Figure 3.- Variation of pitch-jet thrust and moment with chamber pressure for jet discharging into quiescent air. Ambient pressure is 14.78 psia $\left(101.9 \times 10^3 \frac{\text{newtons}}{\text{meter}^2}\right)$.

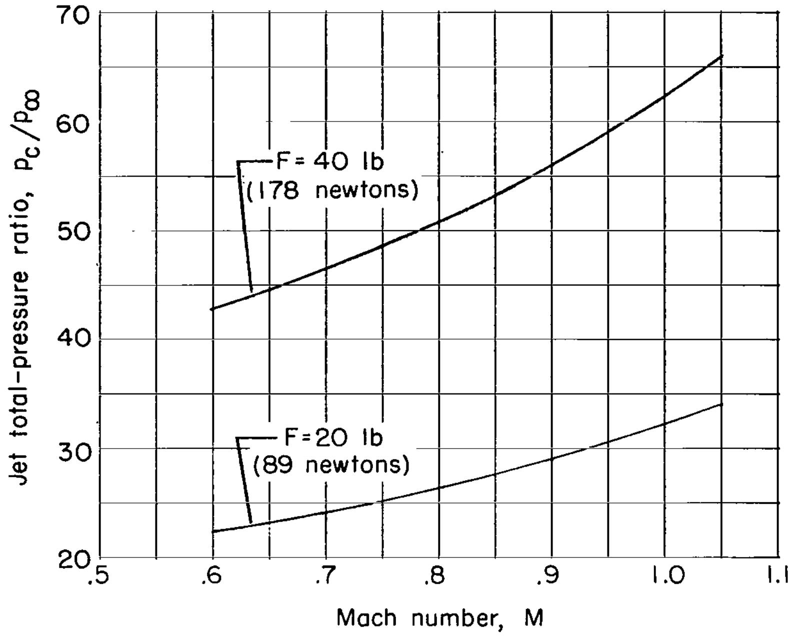

(a) Constant thrust.

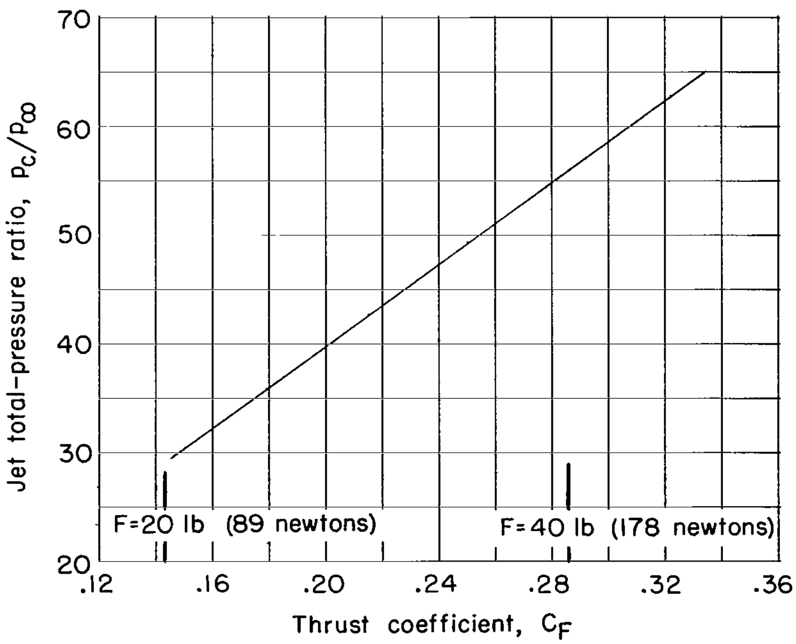

(b) Variable thrust; M = 0.90.

Figure 4.- Variation of jet total-pressure ratio for tests at both constant and variable thrust conditions.

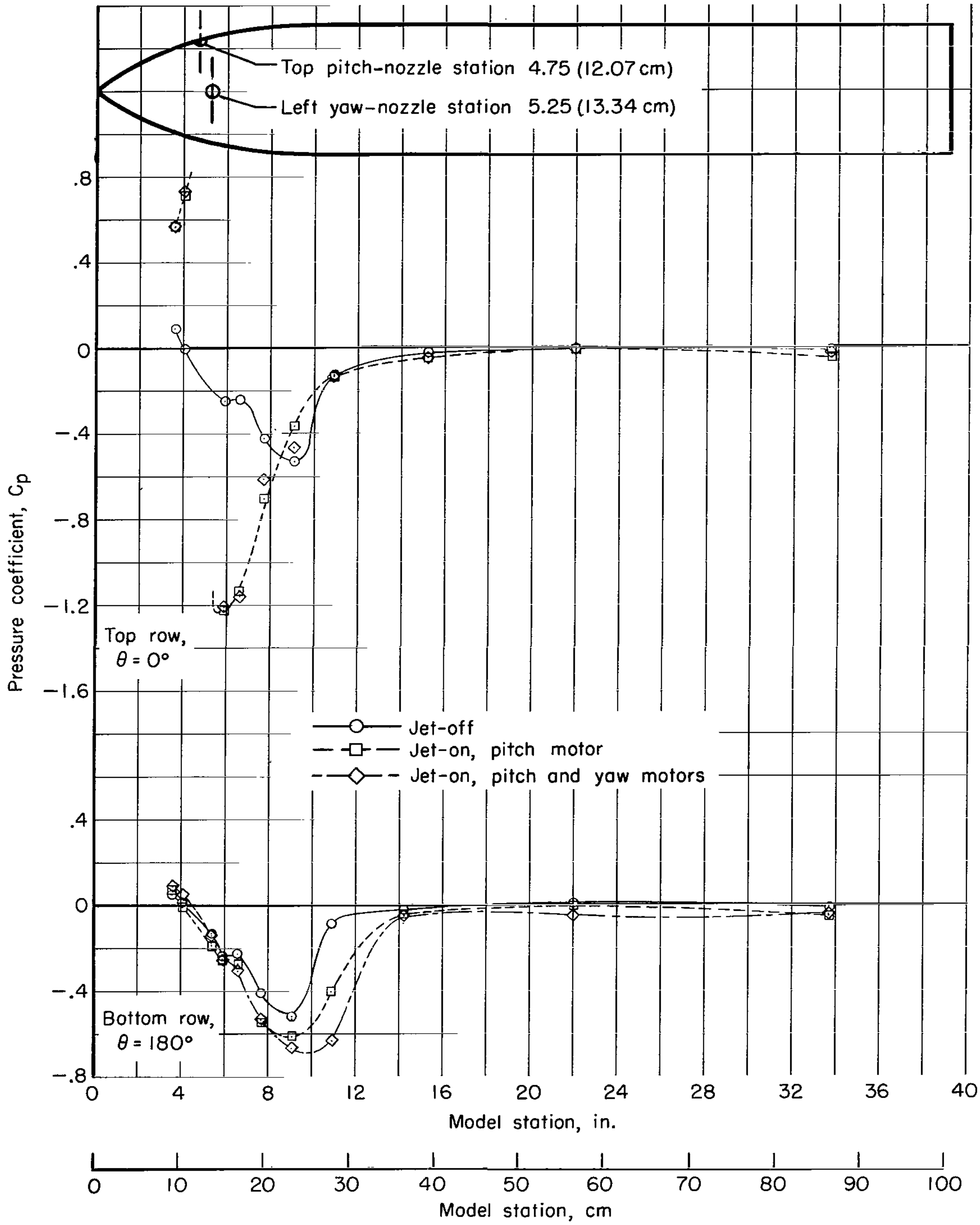

(a) Longitudinal pressure distributions.

Figure 5.- Typical pressure distributions on the model with jets off and with pitch and yaw jets operating at F = 40 lb (178 newtons). M = 0.90; $\alpha = 0^{0}$.

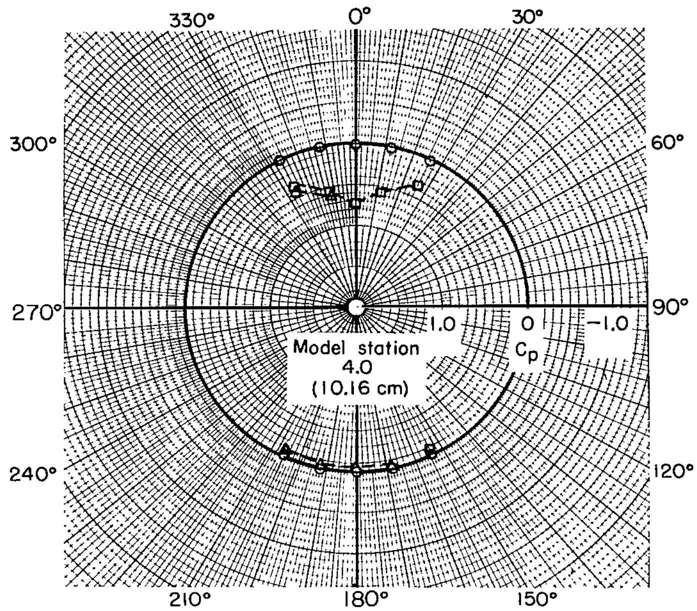

○ Jet-off
□ Jet-on, pitch nozzle at 0°, station 4.75 (12.07 cm)
△ Jet-on, pitch nozzle at 0°, station 4.75 (12.07 cm) plus yaw nozzle at 270°, station 5.25 (13.34 cm)

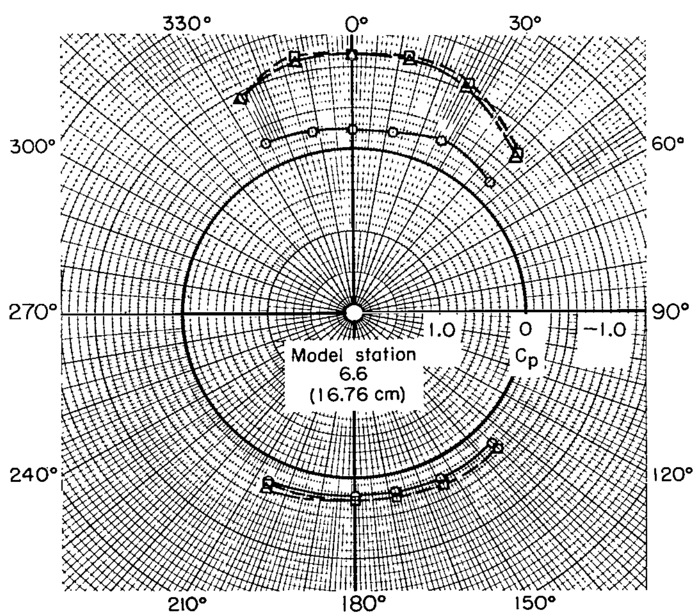

(b) Circumferential pressure distributions.

Figure 5.- Concluded.

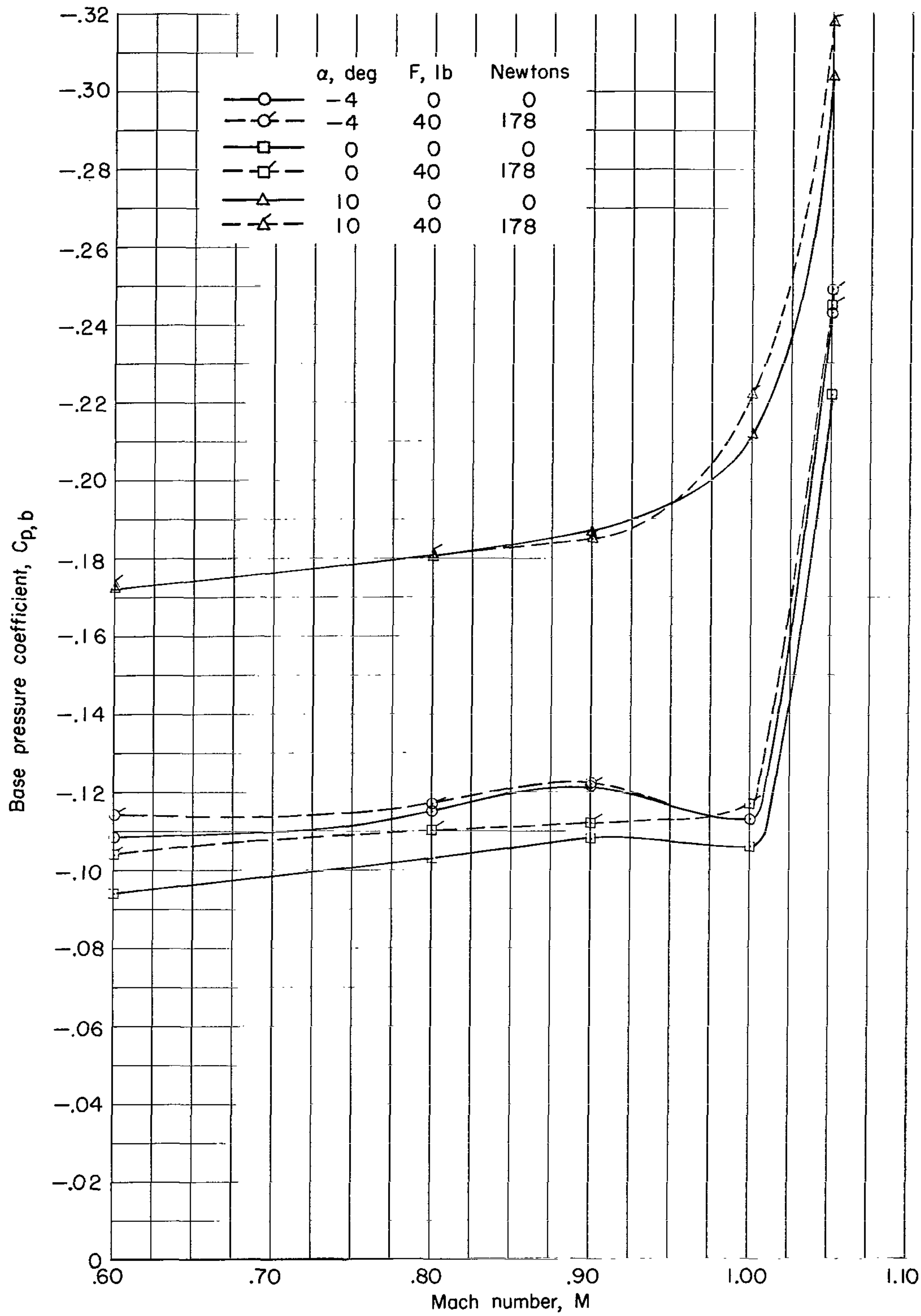

Figure 6.- Effect of pitch-jet operation on model base pressures over the Mach number range.

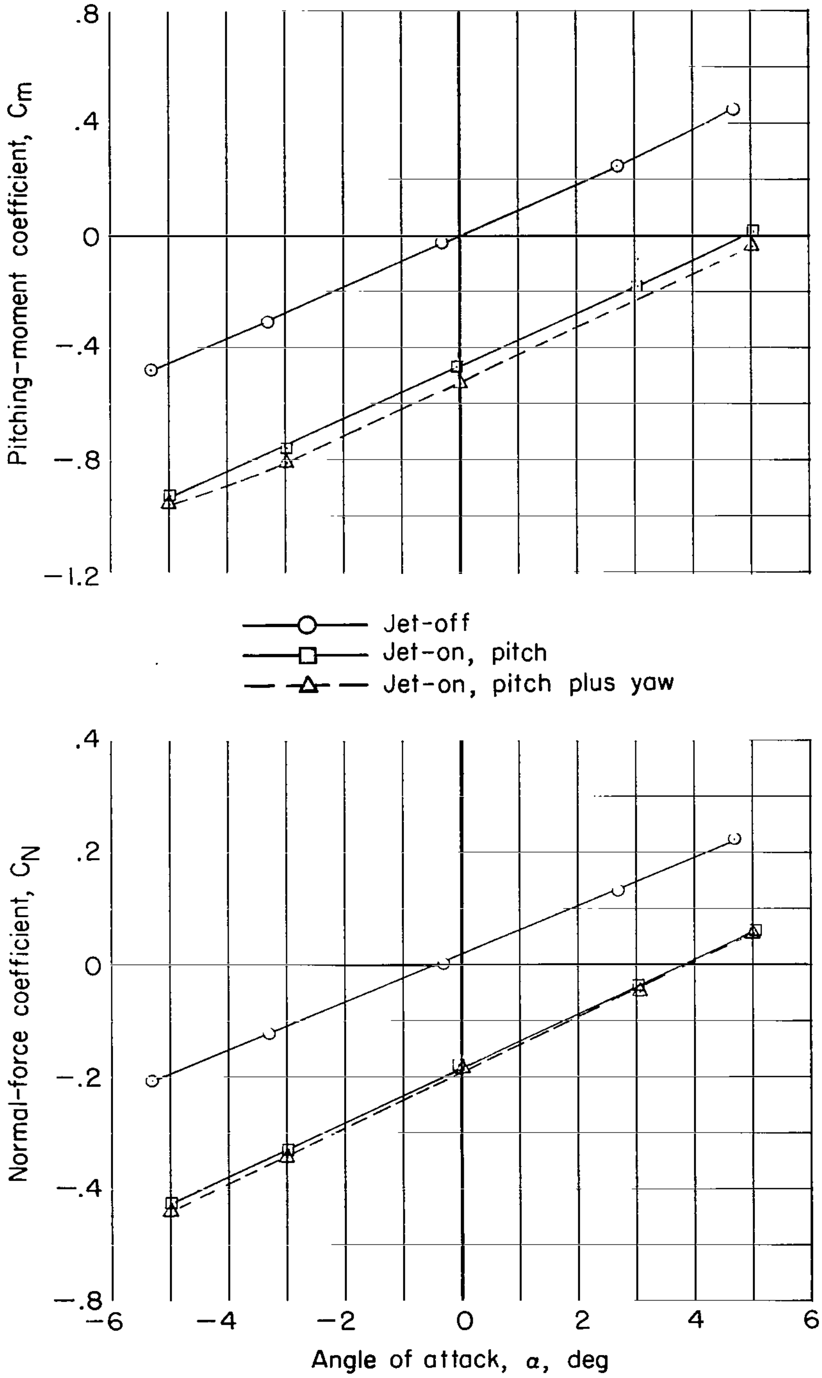

Figure 7.- Comparison of normal-force and pitching-moment coefficients for the pitch jet firing singly and in combination with the yaw jet. F = 40 lb (178 newtons); M = 0.90.

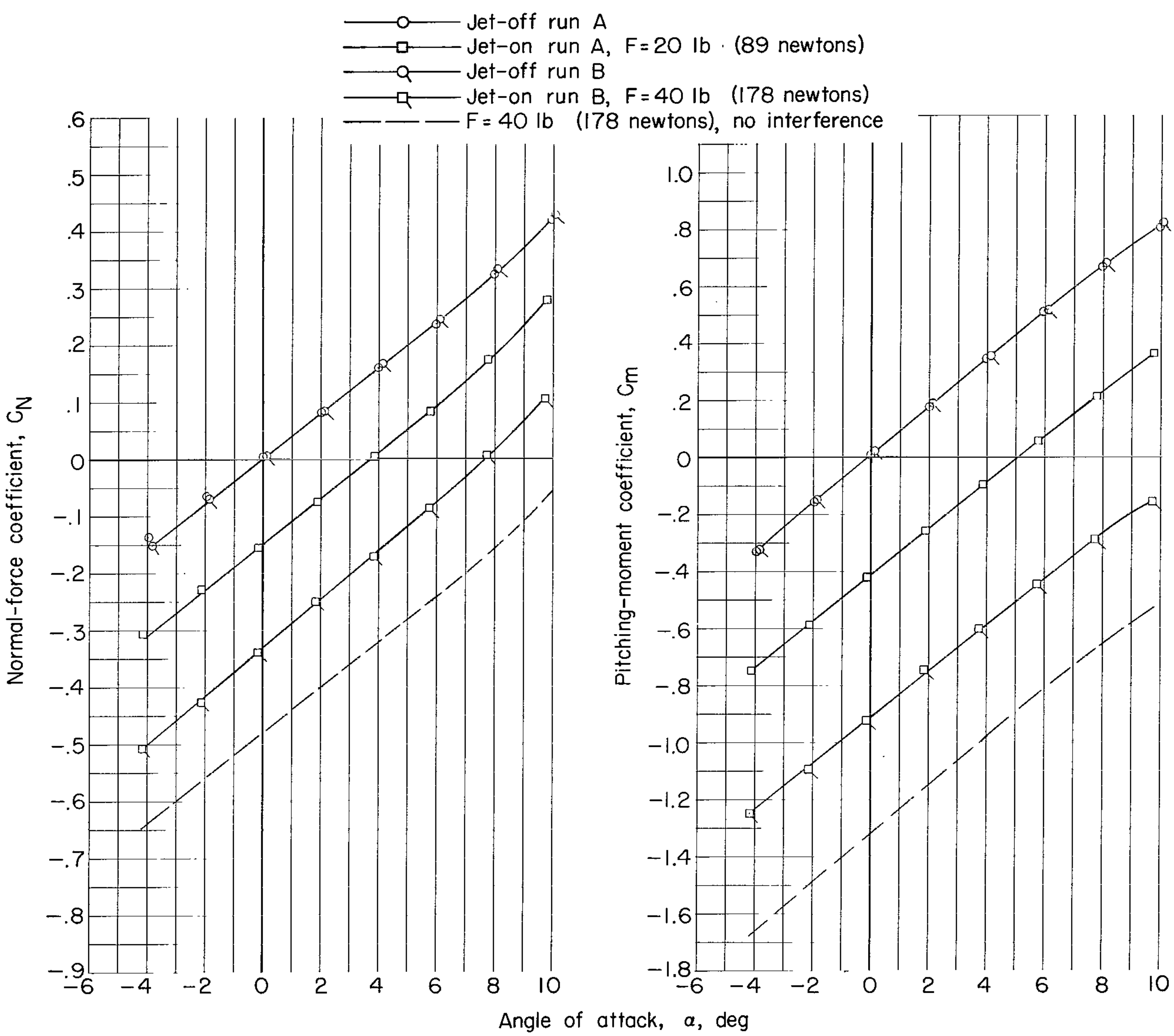

(a) M = 0.60.

Figure 8.- Variation of normal-force and pitching-moment coefficients with angle of attack for pitch jet only.

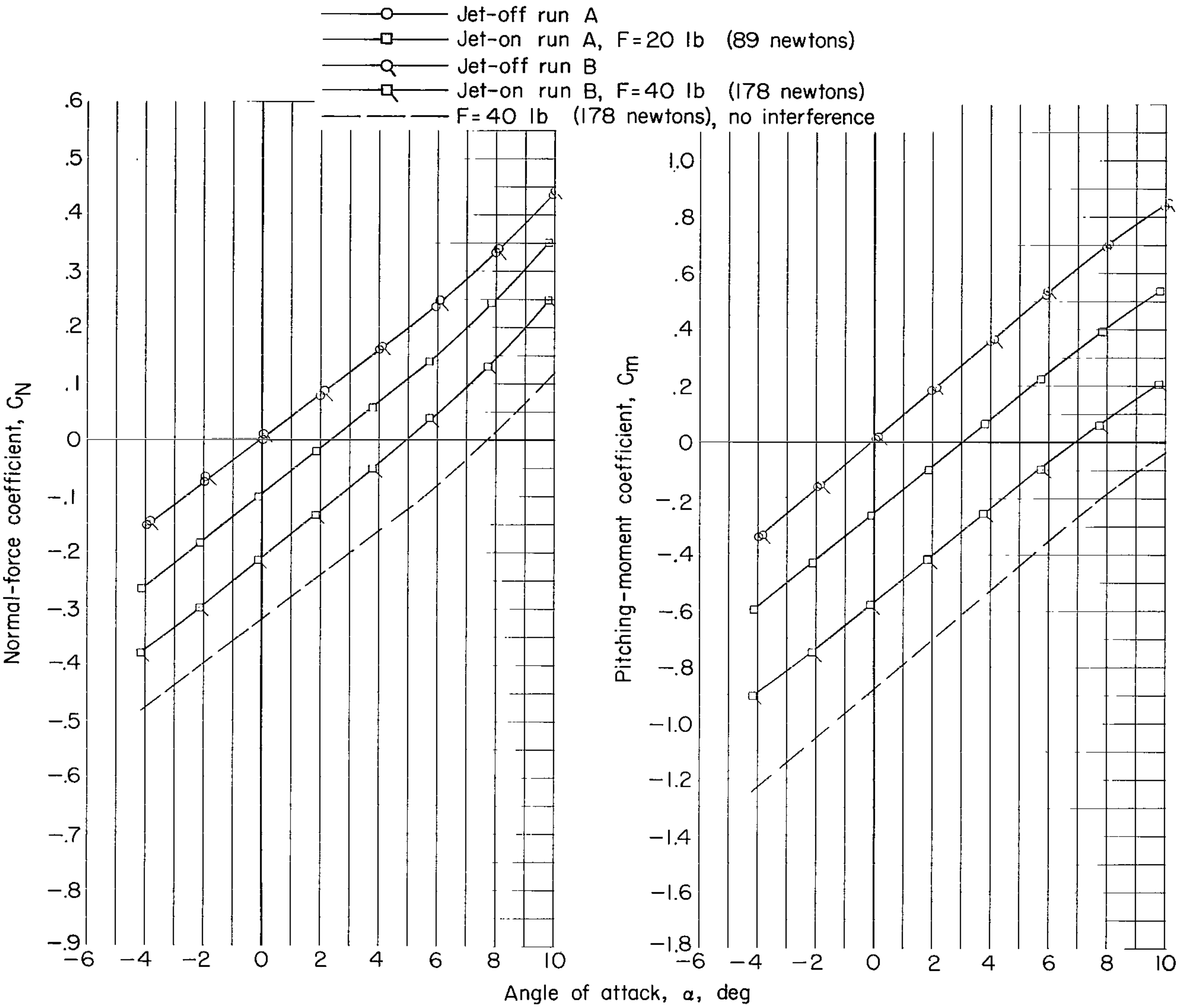

(b) M = 0.80.

Figure 8.- Continued.

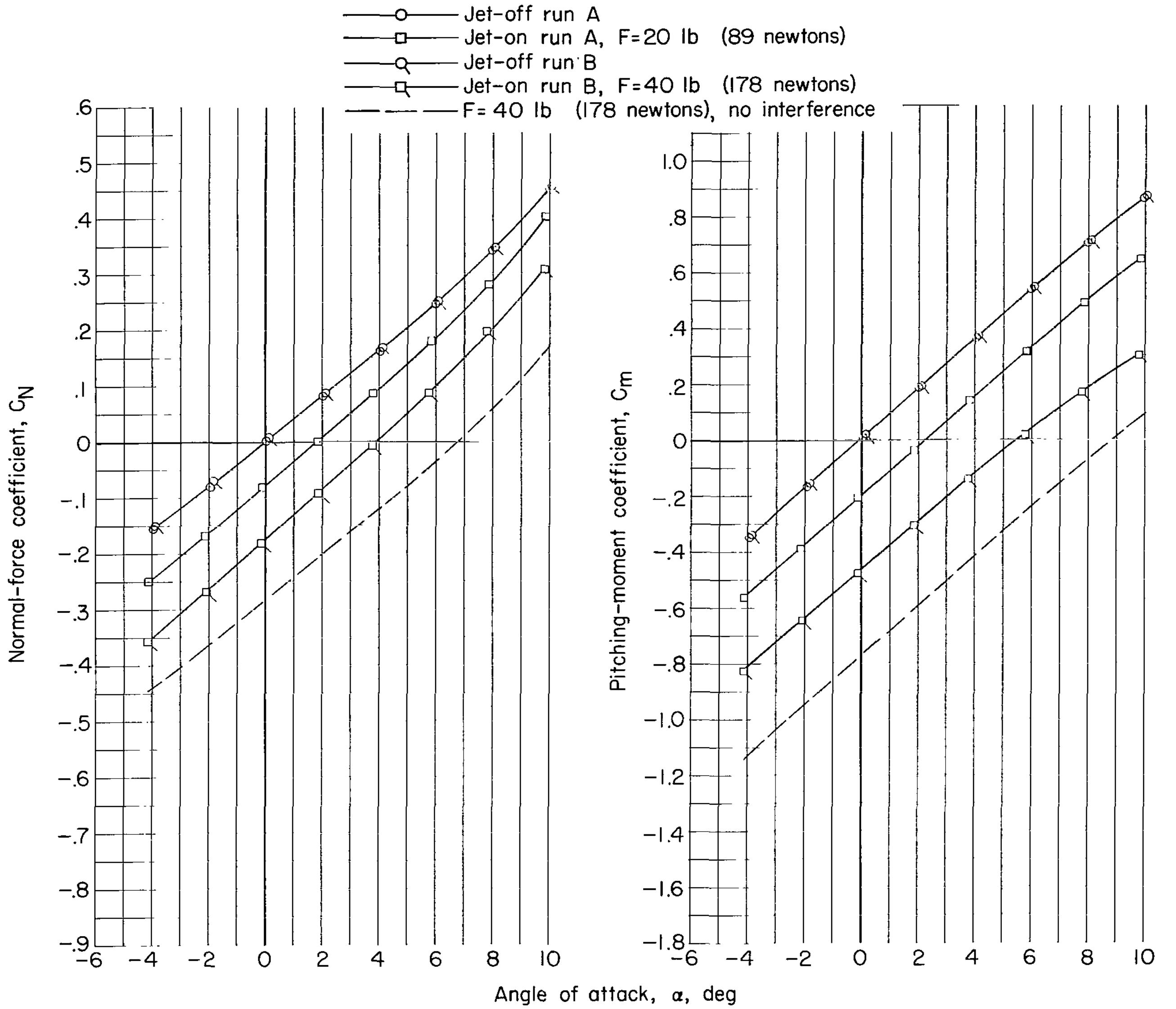

(c) M = 0.90.

Figure 8.- Continued.

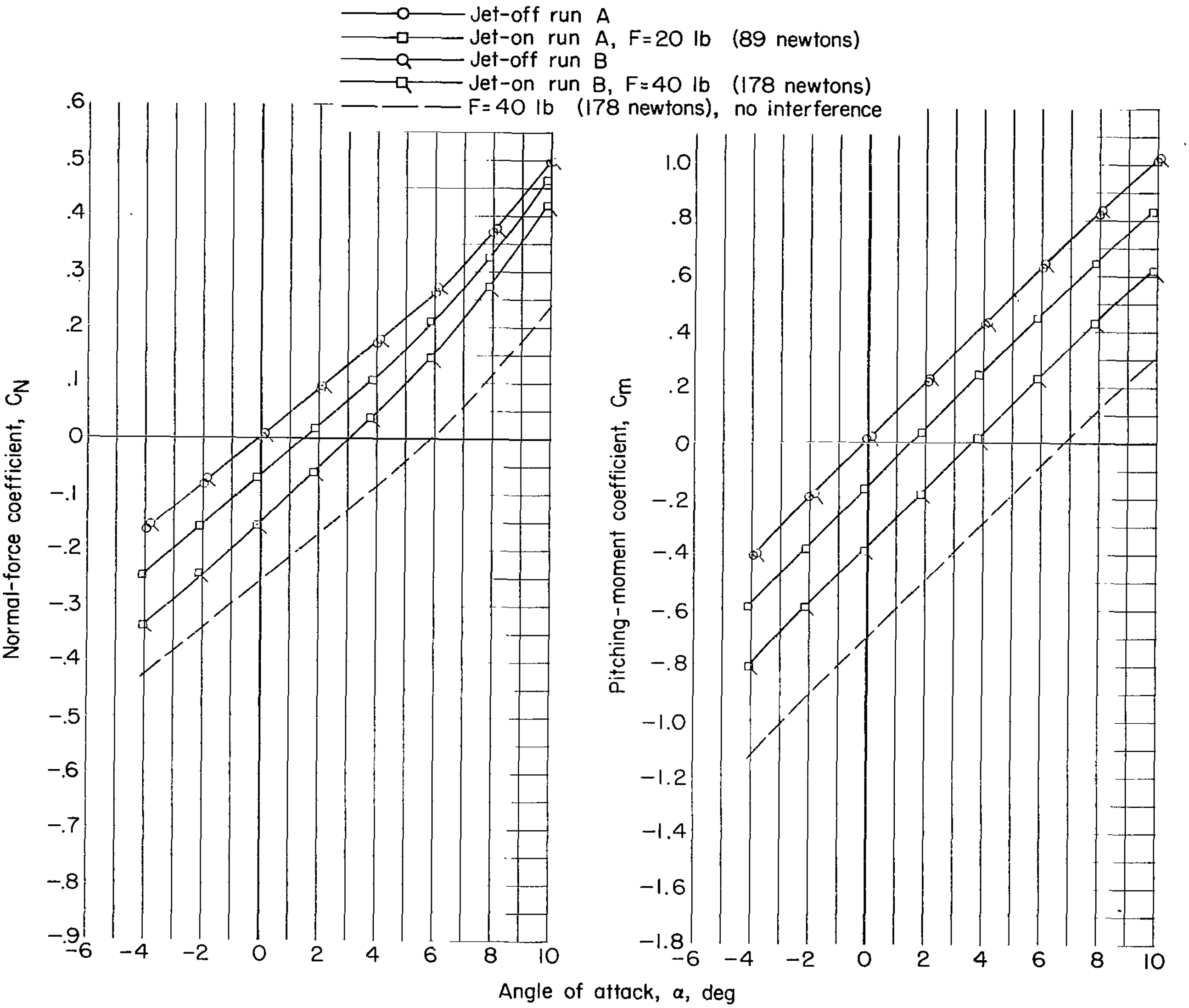

(d) M = 1.00.

Figure 8.- Continued.

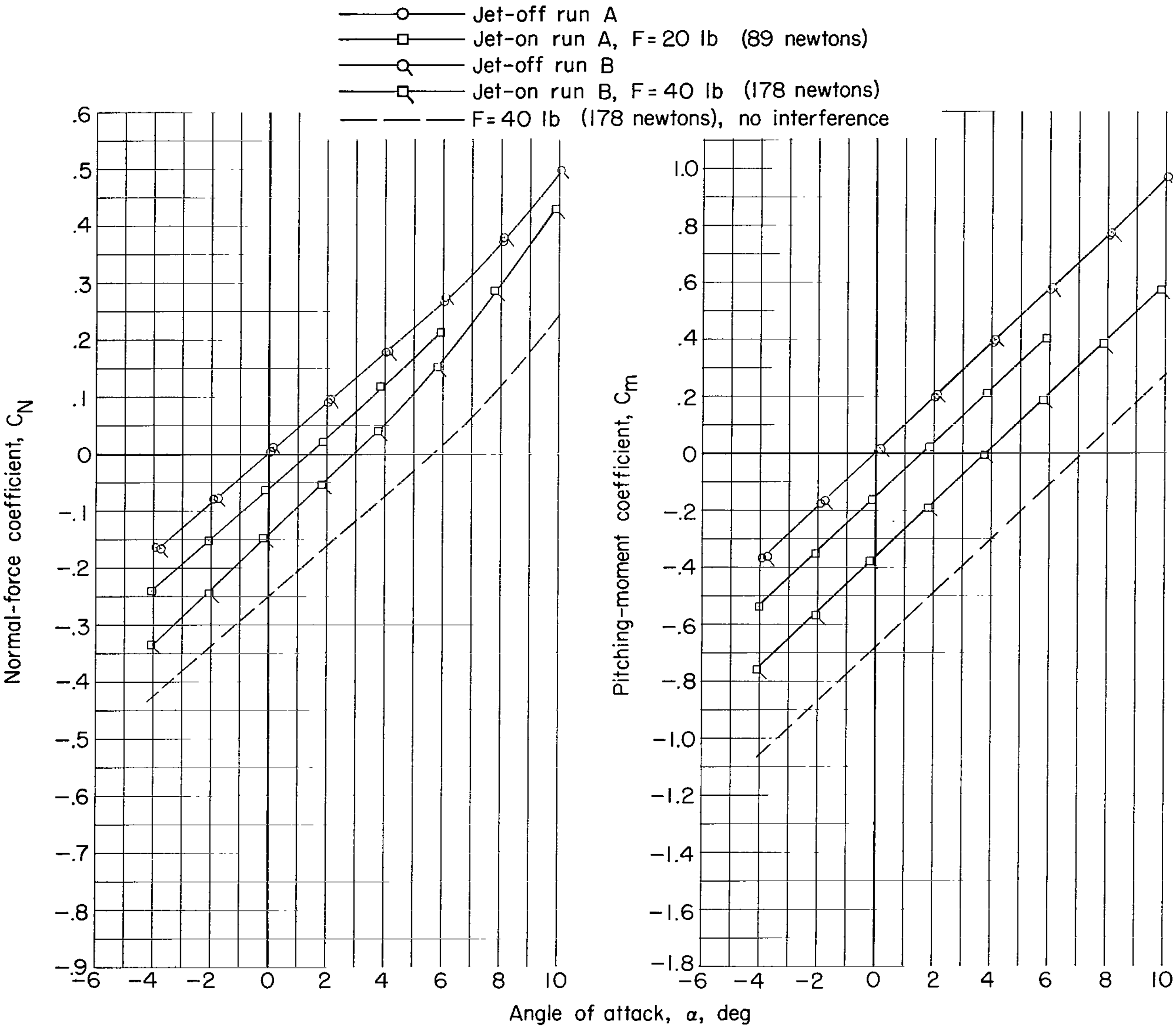

(e) M = 1.05.

Figure 8.- Concluded.

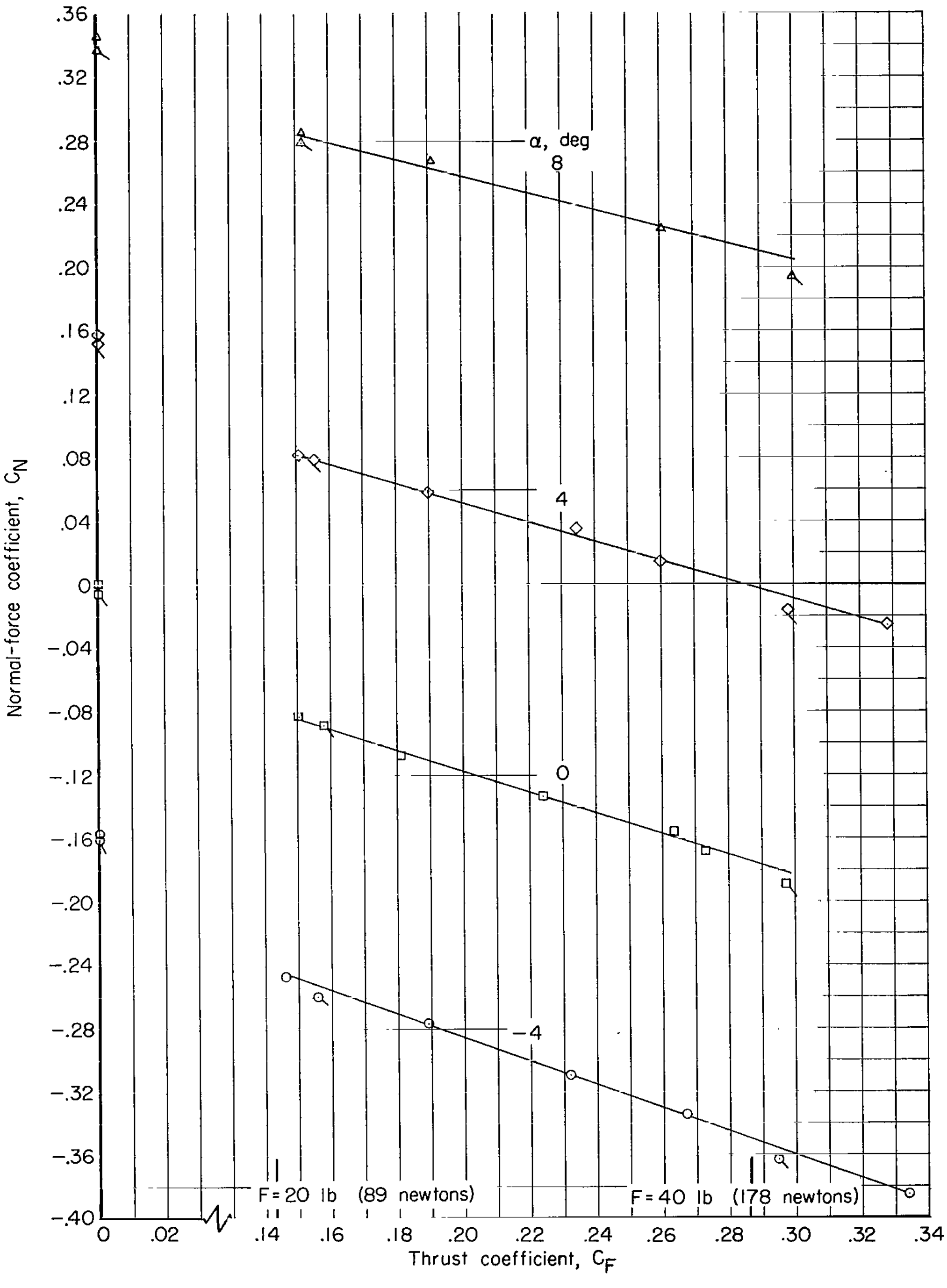

(a) Normal-force coefficient.

Figure 9.- Variation of normal-force and pitching-moment coefficients with pitch-jet thrust coefficient. Tailed symbols indicate repeat data. M = 0.90.

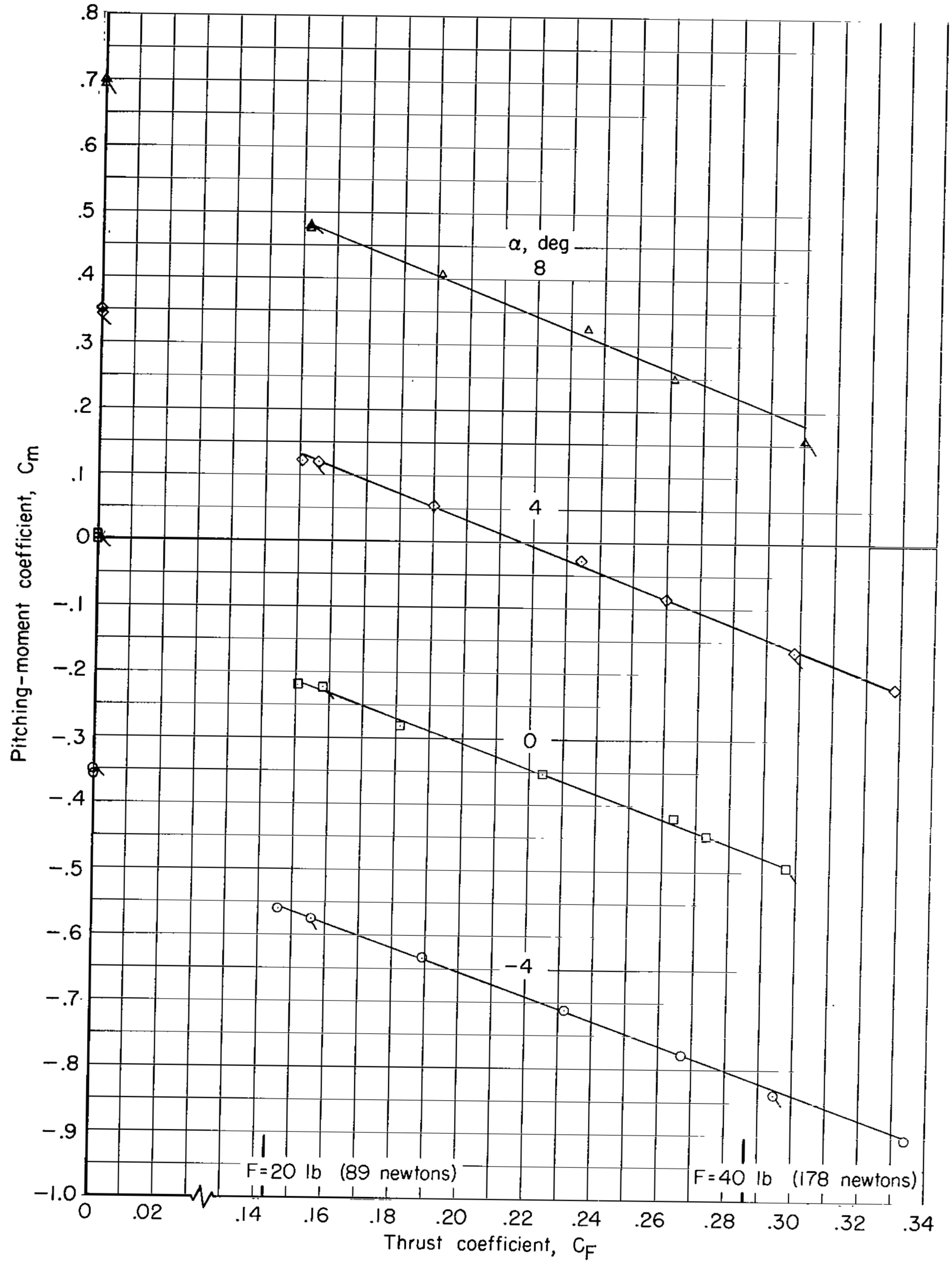

(b) Pitching-moment coefficient.

Figure 9.- Concluded.

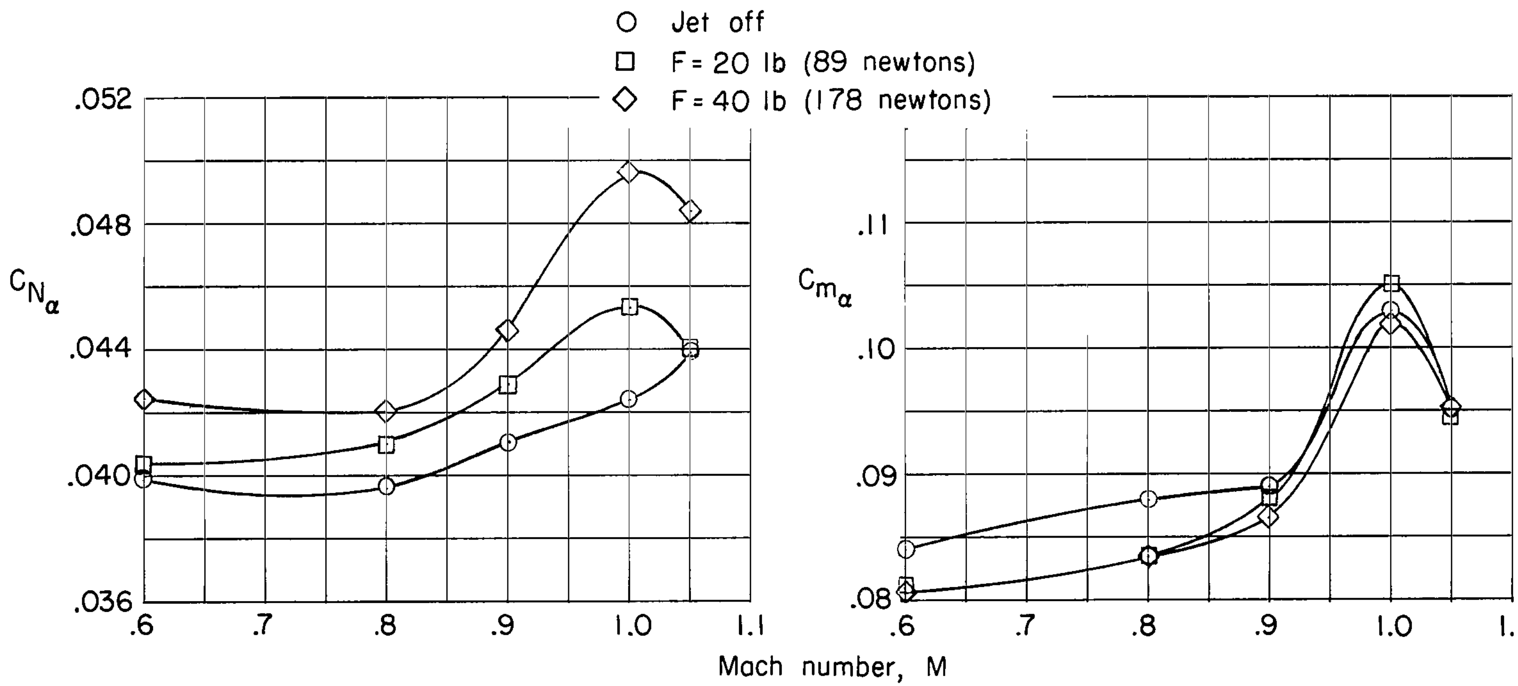

Figure 10.- Slopes of normal-force and pitching-moment curves at $\alpha = 0^0$ with the pitch jet off and operating.

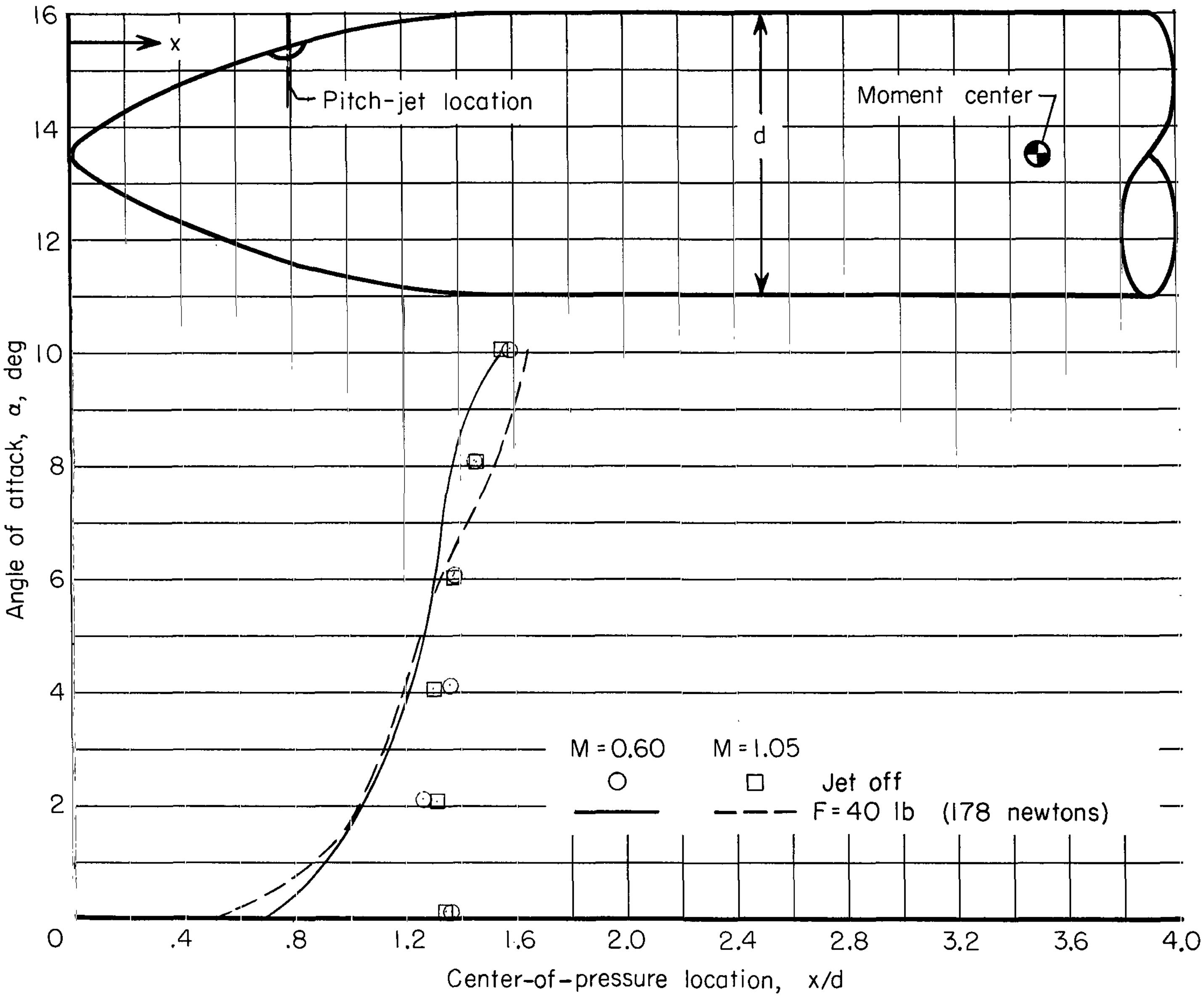

Figure 11.- Effect of induced jet interference on model center-of-pressure location at positive angles of attack. Jet-on data do not include the influence of jet thrust.

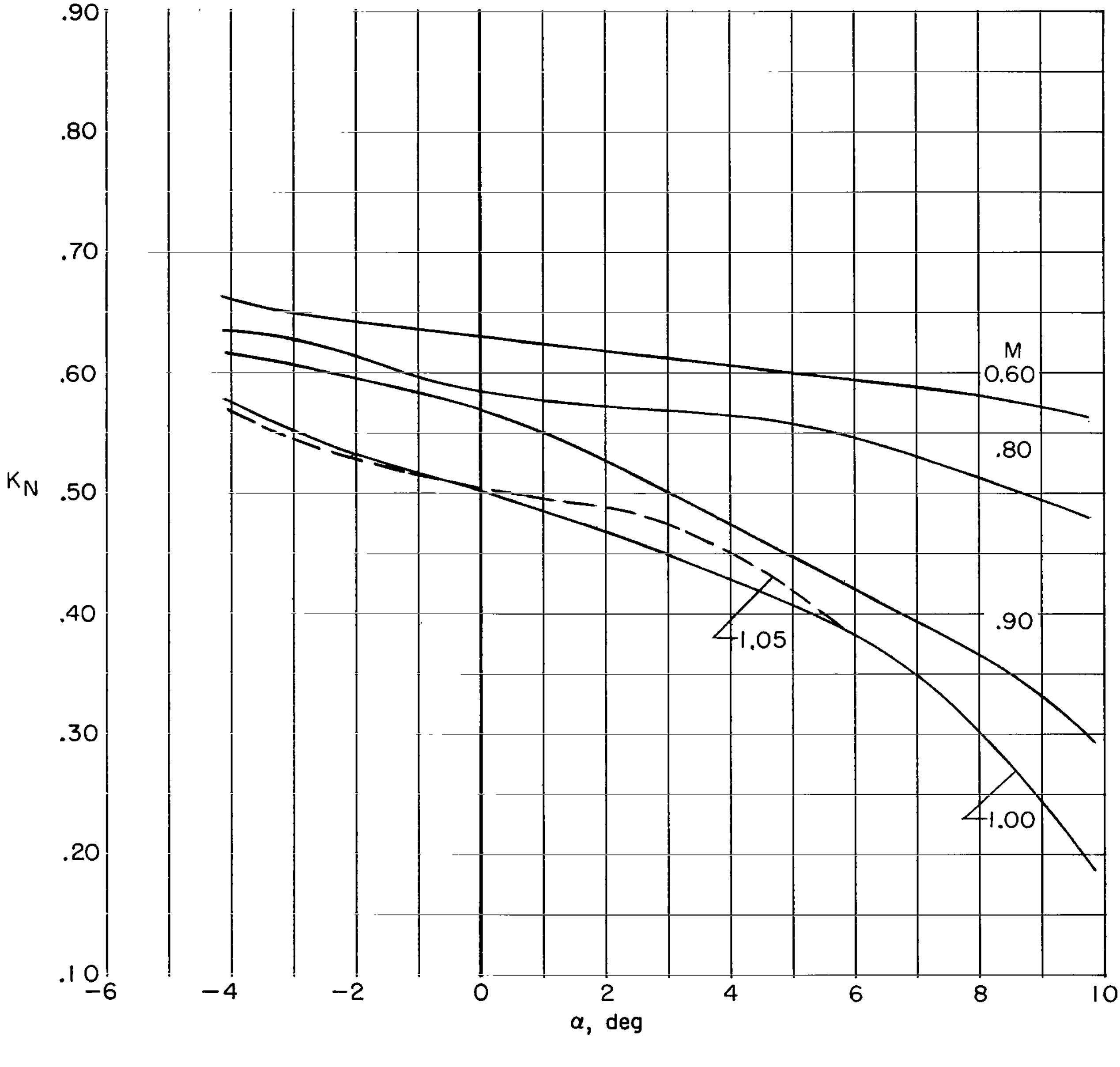

(a) F = 20 lb (89 newtons).

Figure 12.- Variation of jet normal-force effectiveness with angle of attack.

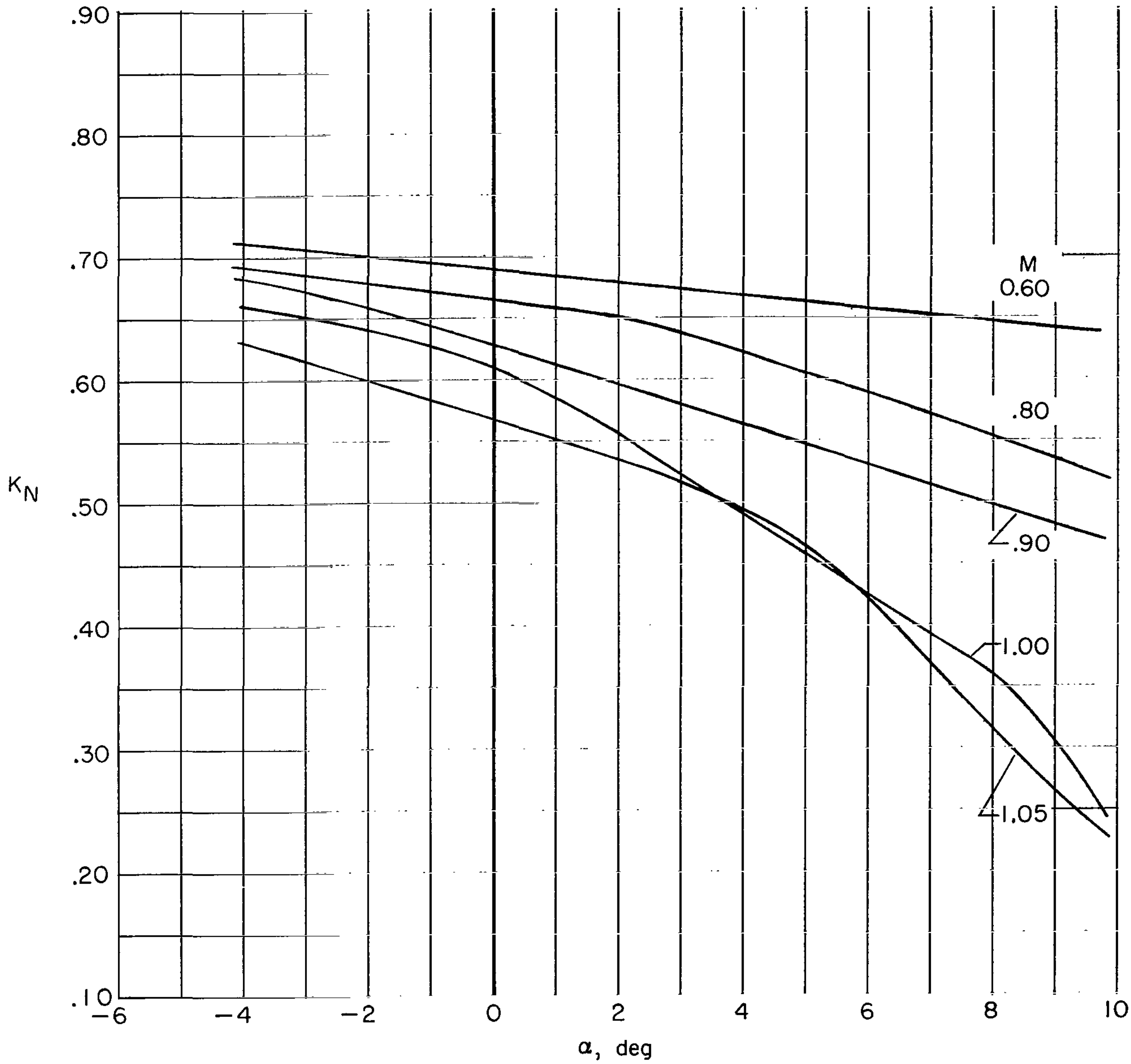

(b) F = 40 lb (178 newtons).

Figure 12.- Concluded.

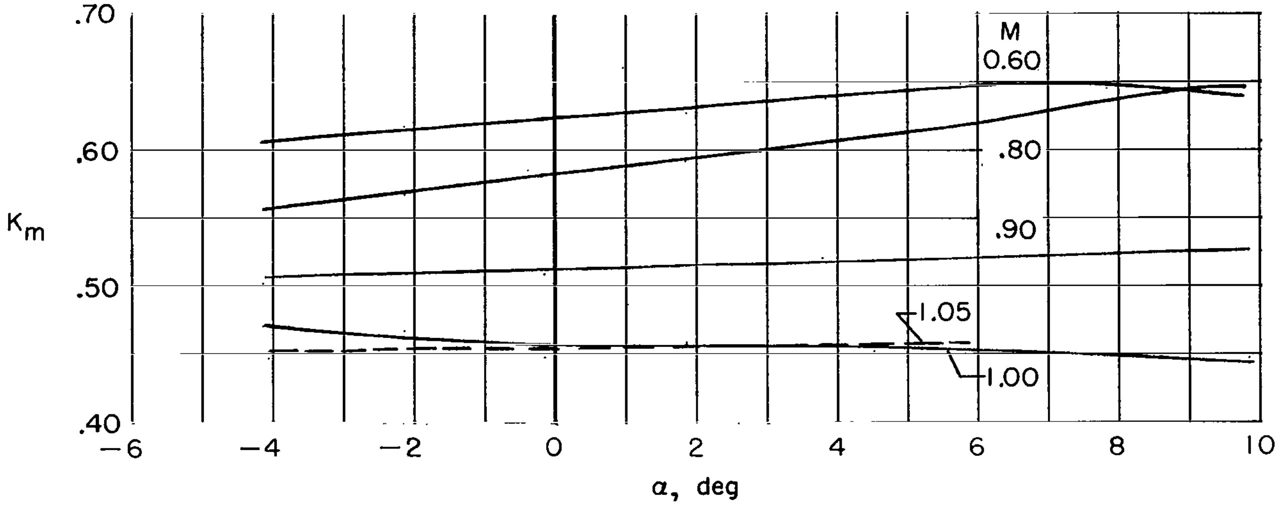

(a) F = 20 lb (89 newtons).

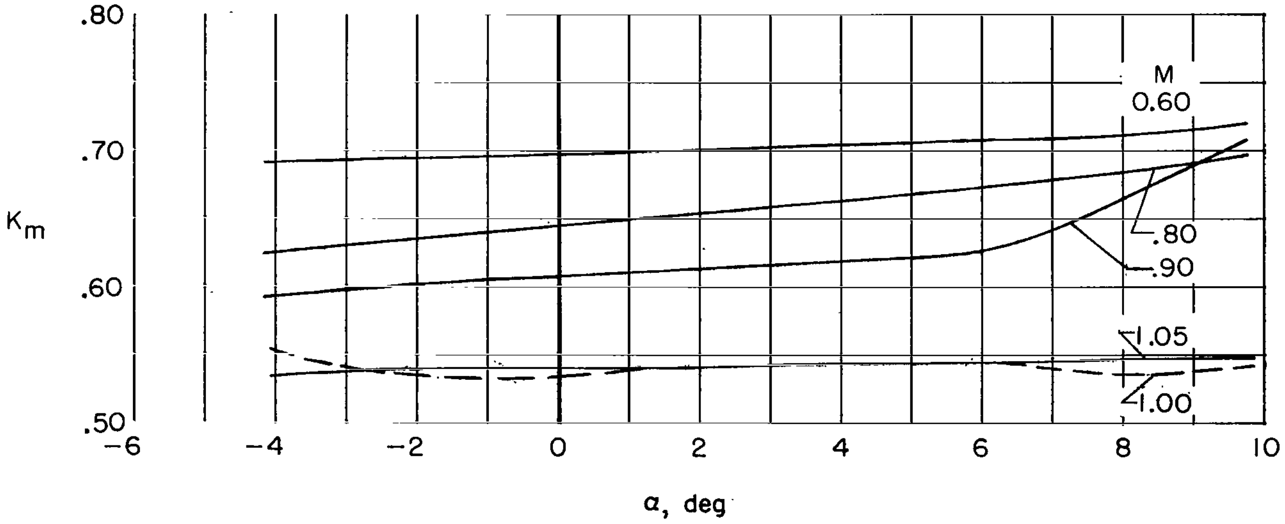

(b) F = 40 lb (178 newtons).

Figure 13.- Variation of jet pitching-moment effectiveness with angle of attack.

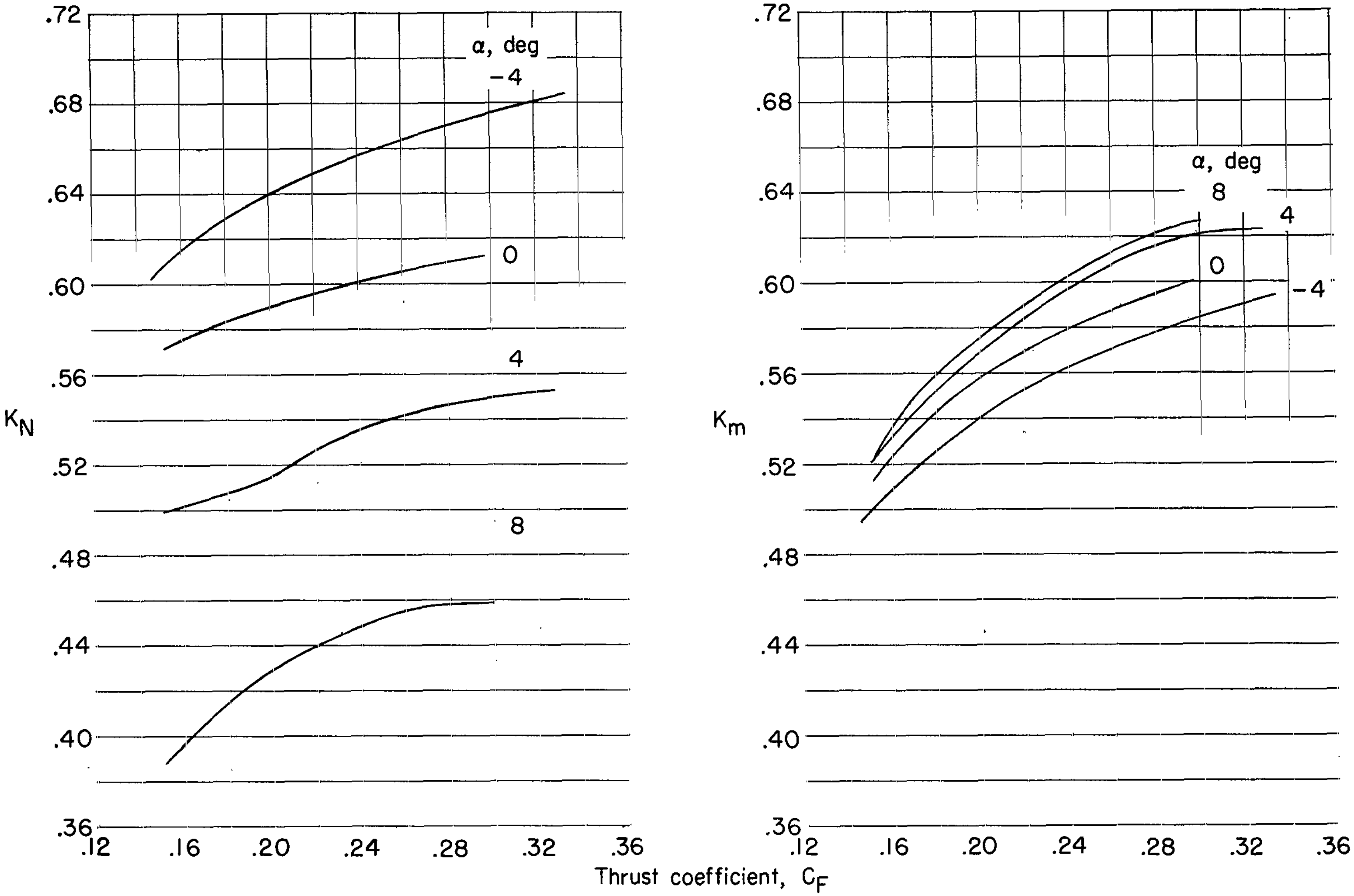

Figure 14.- Influence of thrust coefficient on jet normal-force and pitching-moment effectiveness. M = 0.90.

NASA-Langley, 1967 L-3208

"The aeronautical and space activities of the United States shall be conducted so as to contribute . . . to the expansion of human knowledge of phenomena in the atmosphere and space. The Administration shall provide for the widest practicable and appropriate dissemination of information concerning its activities and the results thereof."

—NATIONAL AERONAUTICS AND SPACE ACT OF 1958

NASA SCIENTIFIC AND TECHNICAL PUBLICATIONS

TECHNICAL REPORTS: Scientific and technical information considered important, complete, and a lasting contribution to existing knowledge.

TECHNICAL NOTES: Information less broad in scope but nevertheless of importance as a contribution to existing knowledge.

TECHNICAL MEMORANDUMS: Information receiving limited distribution because of preliminary data, security classification, or other reasons.

CONTRACTOR REPORTS: Technical information generated in connection with a NASA contract or grant and released under NASA auspices.

TECHNICAL TRANSLATIONS: Information published in a foreign language considered to merit NASA distribution in English.

TECHNICAL REPRINTS: Information derived from NASA activities and initially published in the form of journal articles.

SPECIAL PUBLICATIONS: Information derived from or of value to NASA activities but not necessarily reporting the results of individual NASA-programmed scientific efforts. Publications include conference proceedings, monographs, data compilations, handbooks, sourcebooks, and special bibliographies.

Details on the availability of these publications may be obtained from:

SCIENTIFIC AND TECHNICAL INFORMATION DIVISION

NATIONAL AERONAUTICS AND SPACE ADMINISTRATION

Washington, D.C. 20546